

Heterogeneity and non-linearity of ecosystem responses to climate change in the Qilian Mountains National Park, China

GAO Xiang¹, WEN Ruiyang¹, Kevin LO^{2*}, LI Jie¹, YAN An¹

¹ College of Earth and Environmental Sciences, Lanzhou University, Lanzhou 730000, China;

² Department of Geography, Hong Kong Baptist University, Hong Kong 999077, China

Abstract: Ecosystem responses to climate change, particularly in arid environments, is an understudied topic. This study conducted a spatial analysis of ecosystem responses to short-term variability in temperature, precipitation, and solar radiation in the Qilian Mountains National Park, an arid mountainous region in Northwest China. We collected precipitation and temperature data from the National Science and Technology Infrastructure Platform, solar radiation data from the China Meteorological Forcing Dataset, and vegetation cover remote-sensing data from the Moderate Resolution Imaging Spectroradiometer. We used the vegetation sensitivity index to identify areas sensitive to climate change and to determine which climatic factors were significant in this regard. The findings revealed a high degree of heterogeneity and non-linearity of ecosystem responses to climate change. Four types of heterogeneity were identified: longitude, altitude, ecosystem, and climate disturbance. Furthermore, the characteristics of nonlinear ecosystem responses to climate change included: (1) inconsistency in the controlling climatic factors for the same ecosystems in different geographical settings; (2) the interaction between different climatic factors results in varying weights that affect ecosystem stability and makes them difficult to determine; and (3) the hysteresis effect of vegetation increases the uncertainty of ecosystem responses to climate change. The findings are significant because they highlight the complexity of ecosystem responses to climate change. Furthermore, the identification of areas that are particularly sensitive to climate change and the influencing factors has important implications for predicting and managing the impacts of climate change on ecosystems, which can help protect the stability of ecosystems in the Qilian Mountains National Park.

Keywords: ecosystem resistance; ecosystem stability; climate change; vegetation sensitivity index (VSI); Qilian Mountains National Park

Citation: GAO Xiang, WEN Ruiyang, Kevin LO, LI Jie, YAN An. 2023. Heterogeneity and non-linearity of ecosystem responses to climate change in the Qilian Mountains National Park, China. *Journal of Arid Land*, 15(5): 508–522. <https://doi.org/10.1007/s40333-023-0101-9>

1 Introduction

As the impact of climate change becomes more pronounced and severe, understanding the response of ecosystems to these changes has become crucial (Seddon et al., 2016; Jiang et al., 2017; Morin et al., 2018; Rogora et al., 2018; Liu et al., 2019; Piao et al., 2019; Woolway et al., 2020). Vegetation dynamics, in particular, are important indicators of the impact of global climate change (Qu et al., 2020). As a wide-ranging and persistent disturbance, climate fluctuations

*Corresponding author: Kevin LO (E-mail: lokevin@hkbu.edu.hk)

Received 2022-09-08; revised 2023-01-04; accepted 2023-01-25

© Xinjiang Institute of Ecology and Geography, Chinese Academy of Sciences, Science Press and Springer-Verlag GmbH Germany, part of Springer Nature 2023

substantially affect the overall stability of vegetation and drive changes in vegetation cover (Chen et al., 2019; Huang and Xia, 2019; Shang et al., 2022). In arid and semi-arid regions, climate change has been identified as the primary cause of shifts in vegetation dynamics (Chen et al., 2019; Miao et al., 2021).

The interaction between ecosystems and climate change is very complex owing to the intricate nature of ecosystems, volatility and uncertainty of climate change, and hysteresis of vegetation responses (Malhi et al., 2020). The literature regarding the relationship between climate change and ecosystems presents inconclusive results. Discussions center primarily on the climatic factors driving ecosystem responses and whether the responses exhibit non-linear characteristics (Hillebrand et al., 2020; Kang et al., 2022). A significant portion of current understanding of ecosystem responses to climate change is based on assessments of long-term climate change (Seddon et al., 2016). For instance, on glacial-interglacial timescales, fossil pollen records demonstrate that temperature fluctuations are the primary drivers of forest composition and species distribution, and hydroclimate changes strongly influence the composition and structure of forests (Nolan et al., 2018). These findings show that vegetation and ecosystems are not only vulnerable to climatic factors such as solar radiation, temperature, and precipitation (Xu et al., 2016; Stanimirova et al., 2019; Malfasi and Cannone, 2020; Chen et al., 2021), but their responses are also localized, spatially heterogeneous, and species-specific (Liu et al., 2018; He et al., 2020; Li et al., 2020; Zhou et al., 2020).

The impact of short-term climate variability on ecosystems is not well understood. Compared with long-term climate change, short-term climate variability has different effects on ecosystems. As such, the focus on long-term climate change may ignore the interannual variability in climate and ecosystem sensitivity (Sloat et al., 2018). Most ecosystems appear to be more sensitive to short-term climate extremes than to long-term climate change. Generally, the shorter the duration of the response, the greater the magnitude of the impact (van Rooijen et al., 2015; Zhang et al., 2019; Marchal et al., 2020). For example, sudden changes in solar radiation can influence ecosystems by affecting the interannual variability of the carbon flux (Zhang et al., 2016; Chen et al., 2019). On the one hand, lower solar radiation can cause temperatures to fall below the tolerance limit of trees (Bader et al., 2007); on the other hand, excessive solar radiation can inhibit photosynthesis (Gu et al., 2017). The combined effect of temperature and solar radiation can affect vegetation stability (Huang and Xia, 2019). Climate variability can also indirectly affect ecosystems by regulating biodiversity (García-Palacios et al., 2018; Hisano et al., 2018; Weiskopf et al., 2020). As the occurrence and severity of climate extremes display an upward trend, and are expected to continue in the future, determining the sensitivity of vegetation to climate variability can provide important insight into the interactions between ecosystems and climate change.

Short-term ecosystem stability can be conceptualized in terms of resistance to external disturbances (Cai et al., 2018; Sánchez-Pinillos et al., 2019; Joly et al., 2022; Seixas et al., 2022). Resistance refers to the ability of vegetation to withstand environmental disturbances and has been quantified using the magnitude of the vegetation response to climate disturbances (Kerr et al., 2010; De Keersmaecker et al., 2015). In other words, resistance reflects the ability of an ecosystem to sustain a stable state in the face of changing external conditions. The resistance of the ecosystem to climate variability can be defined as the correlation between the climate and vegetation index. The stronger the correlation is, the less stable the ecosystem is. Therefore, the quantification of vegetation sensitivity is important for understanding ecosystem resistance. To this end, Seddon et al. (2016) proposed the vegetation sensitivity index (VSI), which comprehensively assesses the vulnerability, stability, and response rate of global ecosystems to climate variability. Scholars have applied the indicator system to study the relationship between vegetation and climate in different countries and continents, including China (Zhu et al., 2019; Jiang et al., 2022), central Asia (Yuan et al., 2021), and Africa (Zhao et al., 2019). These scholars have also adjusted the VSI according to local environmental conditions, such as by replacing the original climatic variables with solar radiation and the temperature vegetation dryness index.

In this study, we hypothesized that ecosystem responses to climate change exhibit

heterogeneity and non-linearity. The heterogeneous and non-linear relationship can be explored by analyzing ecosystem responses along latitude and altitude gradient, the non-linear fitting between ecosystem responses to temporal changes of climate variables, and the non-linearity in global and local autocorrelation between ecosystem responses and climate variables. Specifically, the research objectives are to: (1) analyze the heterogeneity of ecosystem stability in different dimensions (longitude, altitude, and ecosystem types); (2) quantitatively evaluate the relationship between ecosystem stability and different climate factors; and (3) provide evidence for non-linear responses of ecosystems to climate change.

2 Study area and methodology

2.1 Study area

This study focuses on the Qilian Mountains National Park (QMNP), which is a sprawling nature reserve located in the semi-arid and arid regions of Northwest China, intersecting the Qinghai-Tibet Plateau, Inner Mongolia Plateau, and Loess Plateau (Fig. 1). With a total area of 50,200 km² and an altitude of 4000–5000 m, the QMNP is an important ecological security barrier, water conservation area, and biodiversity conservation area for China (Gao et al., 2021; Li et al., 2022). The QMNP is the core area of the Qilian Mountains. It has a complex and variable mountain climate and diverse ecosystems with considerable spatial differentiation, making it one of the most sensitive areas to climate change. As such, the QMNP is an ideal testing ground for how ecosystems respond to climate change in semi-arid and arid areas.

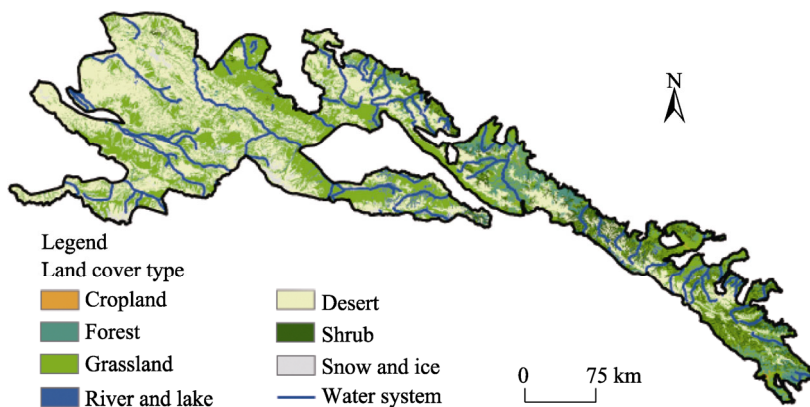


Fig. 1 Overview and land cover type of the study area. Land cover type data are derived from Data Center for Resources and Environmental Sciences, Chinese Academy of Sciences (<https://www.resdc.cn>).

The Qilian Mountains have undergone a prolonged period of warming and increased precipitation. Studies have revealed that the region has experienced the warmest century and the wettest half-century of the last millennium, with an increase in extreme precipitation and high-temperature events. In the QMNP, the mean temperature and precipitation increase by 0.39°C and 8.5 mm every decade, respectively, which are both higher than global and national figures (Wang et al., 2022). Vegetation coverage also shows an increasing trend, the tree line has been significantly raised (Gou et al., 2022), and the vegetation net primary productivity (NPP) is generally increasing (Ma et al., 2022). Regarding the future climate change of the QMNP, it is projected that the temperature in the QMNP will continue to rise, whereas precipitation and evapotranspiration will show a consistent upward trend, and the trend of increasing humidity will slow down (Chen et al., 2021). Liu et al. (2022) predicted that, in the medium-to-long term (2071–2100), the temperature will increase significantly with the largest warming occurring in winter and the smallest in summer. They also forecasted that annual precipitation will increase considerably in winter and spring, whereas the summer and autumn precipitation in the eastern QMNP will decrease substantially. Furthermore, the probability of extreme climate events

(drought) in this area will increase, which may have a profound impact on the ecosystem.

Recent studies on the QMNP have yield inconsistent findings, however, they concur that climate change is the dominant driver of ecosystem changes (Du et al., 2021; Gou et al., 2022). Various arguments propose that temperature, precipitation, or a combination of both, with a lag effect, exert the most prominent control over ecosystems (Qian et al., 2019; Gao et al., 2021; Liu et al., 2021a, b; Du et al., 2022; Ma et al., 2022). In general, there are several competing explanations for vegetation and ecosystem changes in the Qilian Mountains, and there is a lack of research on the relationship between climate change and ecosystem stability.

2.2 Data sources

2.2.1 Climatic data

We chose to study a span of 20 years (2000–2019). The cumulative impact of climate change over the past 20 years is sufficient to provide a comprehensive understanding of ecosystem resistance to climate variability. The precipitation and temperature data were obtained from the National Science and Technology Infrastructure Platform of the National Earth System Science Data Center (<http://www.geodata.cn>). Solar radiation data were acquired from the China Meteorological Forcing Dataset (<http://data.tpdc.ac.cn>). We processed the data on monthly and annual time scales and resampled the spatial resolution to 1 km (i.e., one pixel represented an area of 1 km×1 km on the ground).

2.2.2 Vegetation cover remote sensing data

Moderate Resolution Imaging Spectroradiometer (MODIS)/Terra Vegetation Indices 16-Day L3 Global 250m SIN Grid (MOD13Q1) is a 16-d synthetic vegetation index, including the normalized difference vegetation index (NDVI) and enhanced vegetation index (EVI). This product contained atmospherically corrected bidirectional surface reflectance masked for water, clouds, heavy aerosols, and cloud shadows. Furthermore, it uses the blue band to remove residual atmospheric effects caused by aerosols and subpixel thin clouds. Using the Google Earth Engine platform, we downloaded the EVI images of MOD13Q1 within the border of the QMNP from 2000 to 2019. The EVI layer was then converted into the World Geodetic System (WGS) 1984 projection using data management tools, and the spatial resolution was resampled to 1 km. We further processed the layer into two time series (months and years) for subsequent analysis.

The spatial data of the national ecosystem classification are derived from the China Ecosystem Assessment and Ecological Security Pattern Database (<http://www.ecosystem.csdb.cn/>), which includes various types of ecosystems across the country, provinces, cities, and regions. The dataset includes information, such as the spatial distribution pattern of ecosystems and the areas of different types of ecosystems, with a spatial resolution of 30 m.

The elevation data come from the global 30 m resolution digital elevation model (DEM) data released by the National Aeronautics and Space Administration (NASA). Compared with past Shuttle Radar Topography Mission (SRTM) data, DEM data released by the NASA improve the accuracy of elevation and fill in some missing values.

2.3 Data analysis

2.3.1 Vegetation sensitivity index

VSI is a novel empirical index proposed by Seddon et al. (2016). VSI combines climate and vegetation information to reflect the sensitivity of vegetation to climate variability at a regional or global scale. It is suitable for assessing the climate sensitivity of vegetation over short time-scales (decades). More specifically, VSI explores the relationship between vegetation productivity and the three most relevant climate variables (temperature, precipitation, and solar radiation) on a monthly time-scale. VSI is adopted to represent the resistance of the ecosystem to climate variability. In general, the smaller the VSI value, the stronger the resistance of the ecosystem and the more stable the ecosystem. Based on the Technical specification for investigation and assessment of national ecological status—Ecosystem quality assessment (Ministry of Ecology and Environment of the People's Republic of China, 2021), we divided VSI values into five levels to

represent different degrees of resistance: extremely strong resistance ($VSI < 30.000$), strong resistance ($VSI \in [30.000, 40.000]$), relatively strong resistance ($VSI \in [40.000, 50.000]$)), average resistance ($VSI \in [50.000, 60.000]$)), and weak resistance ($VSI \geq 60.000$).

In this study, VSI was refined to better account for local environmental conditions. The original VSI included three aspects of climate information: temperature, precipitation, and cloud cover. Considering that solar radiation is the main driving factor of vegetation sensitivity in the arid areas of China (Jiang et al., 2022), and the QMNP has a typical mountain climate where cloud cover varies greatly, we replaced cloud cover with solar radiation. In addition, although NDVI is widely used in the literature, it has the drawback of being highly sensitive to atmosphere, soil, and outlier effect. Compared to NDVI, which only shows high-level vegetation conditions throughout the year, EVI is seasonal and has a stronger ability to distinguish vegetation in areas with low vegetation coverage. Furthermore, EVI is more suitable for the analysis of high-density vegetation changes in humid and sub-humid environments. Therefore, we used EVI for VSI calculation. The relative variance of vegetation productivity (using a one-month lag EVI) was compared with the three climate variables (temperature, precipitation, and solar radiation) on a monthly scale to identify regions of strong coupling between vegetation change and climate anomalies.

The basic process of VSI calculation was illustrated in Figure 2. First, a 20×12 matrix was built for each climate factor and EVI data, where 20 represents 20 a from 2000 to 2019, and 12 represents 12 months. The dataset, 960 months of data with 4 variables, was processed, and the "dormant period" areas ($EVI \leq 0.1$) were excluded from the calculation to reduce the impact of sparse or non-existent vegetation cover areas. In addition, one-month lagged monthly EVI data were included as the fourth variable in the regression to investigate the memory effect of vegetation growth. The monthly data were detrended and the results were normalized using stand score (Z-score). Second, we used principal component analysis and multiple linear regression to calculate the regression coefficient of the climate variables for EVI and determine the weight of the impact of each climate factor on vegetation. The weight of each variable was reassigned between 0 and 1 with reference to its minimum and maximum values. Third, we considered the

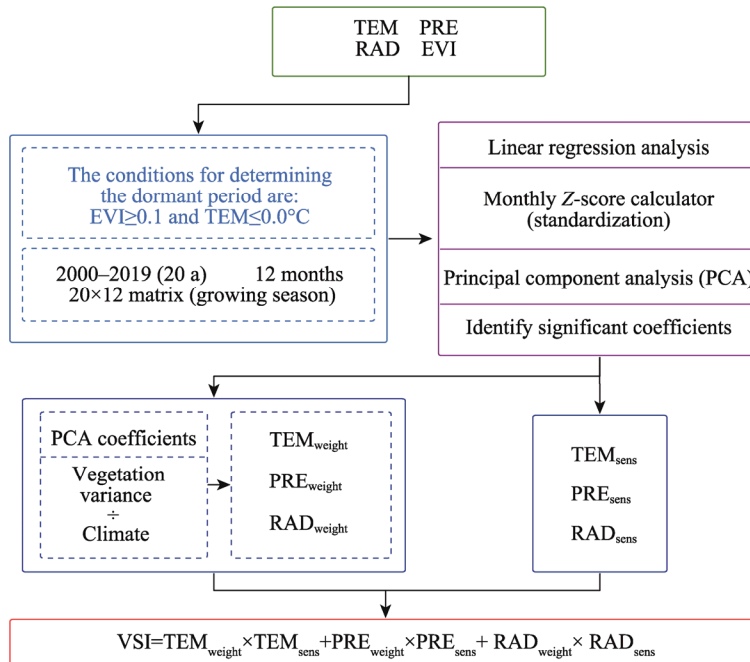


Fig. 2 Flowchart of vegetation sensitivity index (VSI). TEM, temperature; PRE, precipitation; RAD, solar radiation; EVI, enhanced vegetation index; Z-score, stand score; TEM_{weight} , the weight of temperature; PRE_{weight} , the weight of precipitation; RAD_{weight} , the weight of solar radiation; TEM_{sens} , the sensitivity to temperature; PRE_{sens} , the sensitivity to precipitation; RAD_{sens} the sensitivity to solar radiation.

weight distribution ratio of each climate factor and multiplied the weight and variance ratio to obtain a comprehensive VSI reflecting the response of the ecosystem to climate variability. Finally, the results were stretched to 0–100 in MATLAB software. The larger the VSI value, the more sensitive the vegetation to climate variability and the more unstable the ecosystem, and vice versa. The R package for computing VSI can be found in Seddon et al. (2016).

2.3.2 Trend analysis

The trend analysis method models the trend of each grid and reflects the spatial distribution characteristics of vegetation cover changes during different periods. We used this method to model the changes of EVI in the QMNP from 2000 to 2019, and the spatial characteristics of EVI changed with each season. The calculation formula is as follows:

$$\theta_{\text{slop}} = \frac{n \times \sum_{i=1}^n (i \times M_{\text{EVI}_i}) - \sum_{i=1}^n M_{\text{EVI}_i}}{n \times \sum_{i=1}^n i^2 - (\sum_{i=1}^n i)^2}, \quad (1)$$

where θ_{slop} is the vegetation change trend; n is the cumulative number of years from 2000 to 2019; and M_{EVI_i} is the maximum EVI value in the i^{th} year. $\theta_{\text{slop}} > 0$ indicates that the EVI of a pixel exhibits an increasing trend over n years; $\theta_{\text{slop}} < 0$ shows that the EVI of a pixel presents a degrading trend over n years; and $\theta_{\text{slop}} = 0$ implies that the EVI of a pixel remains unchanged. The F -test method was used to analyze the statistical significance of EVI trends. The results were used to express the confidence level of the trend. The formulas for F -test are shown as follows:

$$\hat{y}_i = \text{avg}(y) - \theta_{\text{slop}} \times \text{avg}(x) + \theta_{\text{slop}} \times x_i, \quad (2)$$

$$F = \sum_{i=1}^n (\hat{y}_i - \bar{y})^2 \times (n-2) / \sum_{i=1}^n (y_i - \hat{y}_i)^2, \quad (3)$$

where y is the EVI sequence; $\text{avg}(y)$ is the average of y ; x is the raster data for the year; $\text{avg}(x)$ is the average of x ; x_i and y_i are independent time series subject to normal distribution; \hat{y}_i is the fitted regression value; \bar{y} is the average value for n years; and F is the F -test of equality of variances.

2.3.3 Hurst index

The Hurst index describes the dependence degree of a sequence over a long period (Zhang et al., 2022), and can assess whether future changes in vegetation are persistent. In order to analyze the future trends of vegetation cover changes in the QMNP, we used the rescaled range analysis method to calculate the Hurst index of EVI changes during the vegetation growing season. Assuming that n exists in a time series for any positive integer, there are cumulative deviation ($X_{(t,n)}$), range ($R_{(n)}$), and standard deviation ($SD_{(n)}$) that satisfy the following conditions, indicating that the Hurst phenomenon is present in the analyzed time series, the formulas are as follows:

$$\overline{\text{EVI}_{(t)}} = \frac{1}{n} \sum_{t=1}^n \text{EVI}_{(t)}, \quad (4)$$

$$X_{(t,n)} = \sum_{t=1}^n (\text{EVI}_{(t)} - \overline{\text{EVI}_{(t)}}), \quad (5)$$

$$R_{(n)} = \max X_{(t,n)} - \min X_{(t,n)}, \quad (6)$$

$$SD_{(n)} = \sqrt{\frac{1}{n} \sum_{t=1}^n (\text{EVI}_{(t)} - \overline{\text{EVI}_{(t)}})^2}, \quad (7)$$

$$\frac{R_{(n)}}{SD_{(n)}} = (cn)^H, \quad (8)$$

where t is the study time sequence; $\text{EVI}_{(t)}$ is the time series of EVI; $\overline{\text{EVI}_{(t)}}$ is the average of $\text{EVI}_{(t)}$; $\max X_{(t,n)}$ is the maximum value of cumulative deviation; $\min X_{(t,n)}$ is the minimum value of cumulative deviation; c is the intercept of the regression equation; and H is the Hurst index. When $0.0 < H < 0.5$, the future trend is opposite to the past change. When $H=0.5$, the future trend is

independent of past change. When $0.5 < H < 1.0$, the future trend is consistent with past changes; the larger the H , the stronger the continuity.

3 Results

3.1 Climate and vegetation changes in the QMNP

The annual average temperature of the QMNP from 2000 to 2019 was -5.10°C with a slightly rising moving average. The average temperatures in spring, autumn, and winter displayed upward trends, with the greatest increase observed in spring. The average annual precipitation was 300.0 mm with an increasing moving average. The annual precipitation fluctuated significantly. The rate of increase in precipitation was highest in summer, followed by autumn, whereas spring and winter precipitation decreased slightly over the years. The average annual solar radiation was 1821 MJ/m^2 . The solar radiation level increased significantly in general but decreased slightly in autumn.

From 2000 to 2019, the EVI of the QMNP increased slowly, with abnormally high values in 2005, 2012, and 2018 and low values in 2004 and 2014. The average EVI in spring, summer, and autumn increased, whereas the average EVI in winter decreased slightly (Fig. 3). The F -test was conducted on the results of EVI trend analysis. The critical value was 4.14 at the 5% level. Based on the results of the trend analysis and F -test, we divided the changes in EVI into four categories:

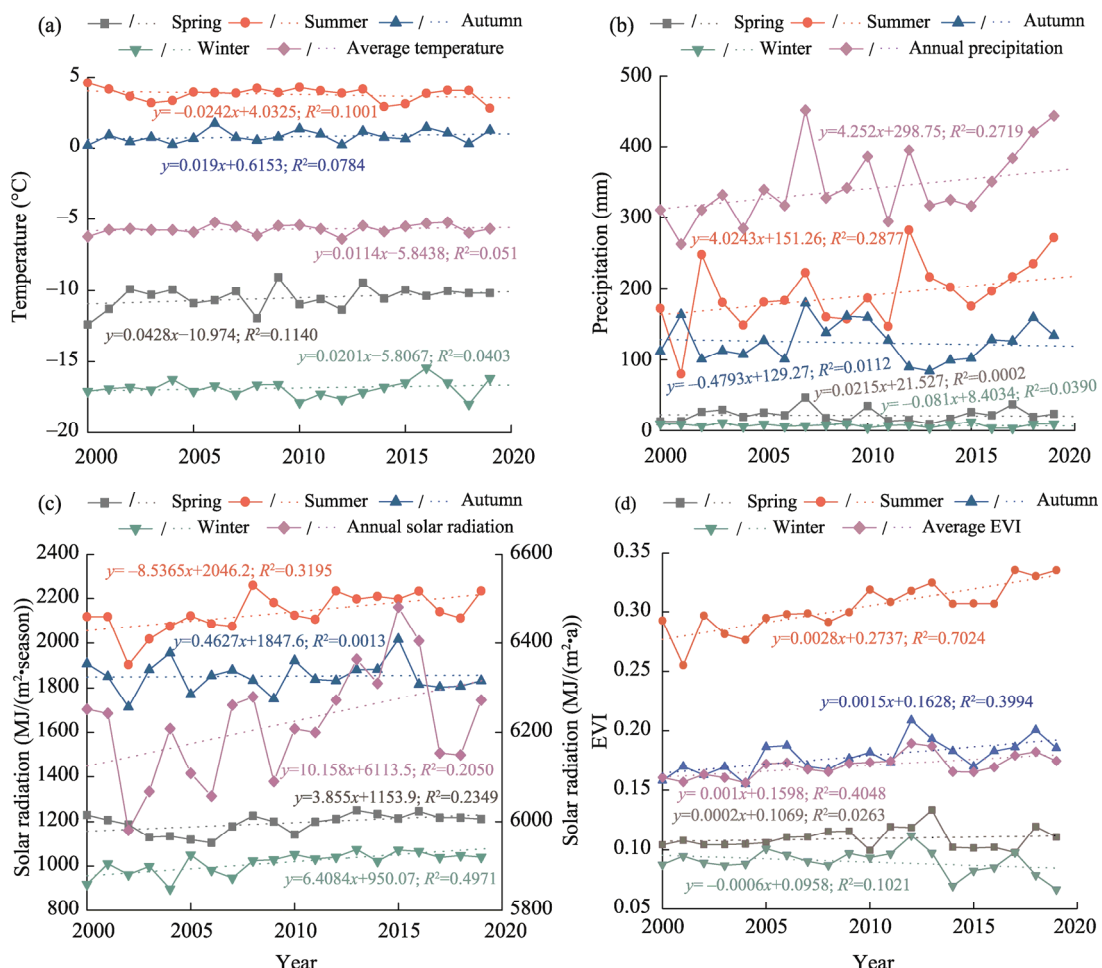


Fig. 3 Changes of temperature (a), precipitation (b), solar radiation (c), and EVI (d) in the Qilian Mountains National Park (QMNP) from 2000 to 2019. The dotted lines represent the linear trends.

significant increase, non-significant increase, significant decrease, and non-significant decrease. From 2000 to 2019, an area of 47,000 km² in the QMNP experienced an increase in EVI, accounting for 93.70% of the total area. In which, 30,600 km² area exhibited a significant increase. Approximately 3160 km² of the area experienced a decrease in the EVI, accounting for 6.30% of the total area. The area where the EVI decreased significantly was approximately 130 km².

The spatial changes in EVI can be analyzed together with the Hurst index to shed light on the future trends of vegetation changes. As shown in Figure 4, the average Hurst index of the QMNP was 0.575, and most areas had a value of Hurst index of 0.500–0.600 (weak persistence, 35.26% of the total area) and 0.600–0.800 (medium persistence, 38.89% of the total area). Therefore, it can be predicted that vegetation coverage in the QMNP will continue to improve.

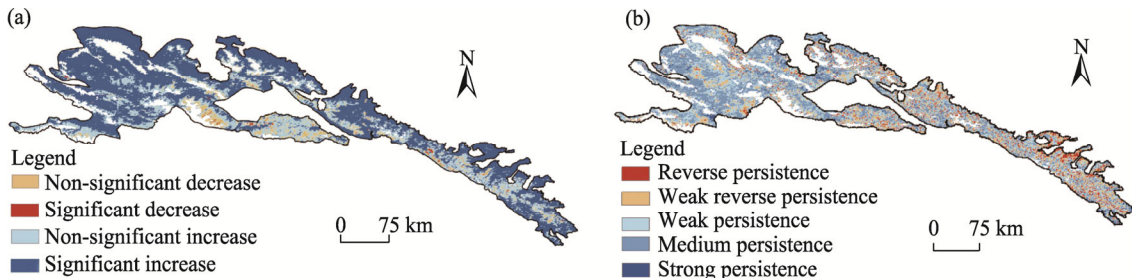


Fig. 4 Spatial patterns of EVI (a) and the Hurst index (b) in the QMNP from 2000 to 2019

3.2 Ecosystem resistance to climate variability in the QMNP

We conducted spatial analysis based on the overall VSI distribution at the pixel level. The median VSI value was 34.693, which was mainly concentrated between 25.000 and 40.000, and the area corresponding to VSI values less than 35.000 accounted for 51.57% of the total area. Pixels with a VSI value less than 25.000 accounted for 11.74% of the total area. This indicated that the ecosystems in the QMNP had relatively high resistance to climate variability over the past 20 years.

3.2.1 Longitudinal heterogeneity of ecosystem resistance

To accurately analyze the geographical differentiation of ecosystem resistance, we divided the QMNP into three sections according to longitude: the west section (95°–98°E), the middle section (98°–100°E), and the east section (100°–103°E). Spatially, the areas with strong resistance were mainly located on the western edge and central-eastern area of the QMNP. Pixels with a VSI value greater than 50.000 accounted for 16.18% of the total area and were mainly distributed on the eastern and western edges of the QMNP (Fig. 5). This indicated that the ecosystems in these areas were more sensitive to climate variability and the ecosystem resistance was weak.

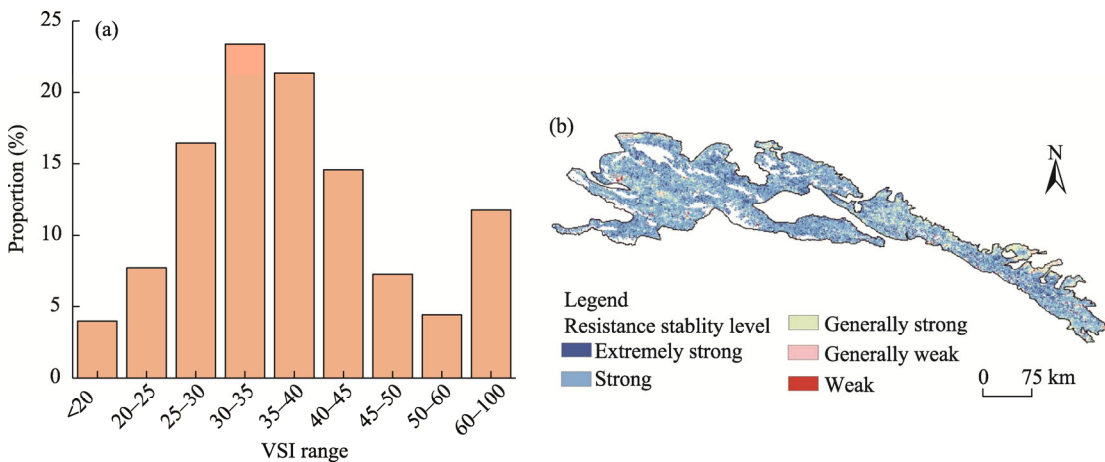


Fig. 5 VSI distribution frequency histogram (a) and spatial differentiation of ecosystem resistance in the QMNP (b)

3.2.2 Altitudinal heterogeneity of ecosystem resistance

In this study, the DEM of the QMNP was resampled into $1\text{ km} \times 1\text{ km}$ pixels, and the QMNP was divided into 41 altitude intervals at 100 m intervals. In ArcMap software, the altitude interval and VSI spatial information were superimposed, and a spatial extraction tool was used to extract the average VSI value of each altitude interval. Figure 6 demonstrated significant altitudinal heterogeneity in the degree of resistance to climate variability. In the 2700–4700 m altitude range, the resistance increased with increasing altitude. Forest grasslands, subalpine shrub meadows, and alpine meadows were distributed in this range. The vegetation coverage, biodiversity, and overall stability in this range were relatively high. Areas with an altitude of less than 2700 m and greater than 4700 m were small, and the average VSI value was easily affected by the maximum and minimum values. Compared with the VSI of other altitude ranges, the contrast was large and not suitable for comparison. Areas below 2700 m above sea level were mostly desert steppes and mountain deserts, the climate was relatively arid, precipitation was low, the influence of climate fluctuation was large, and the resistance of the ecosystem was weak. The tundra zone was located above 4700 m. The vegetation in this region was stable, as it was sparsely distributed with flat cushion-shaped plants and dense tomentose that have strong resistance to cold, frost, and drought.

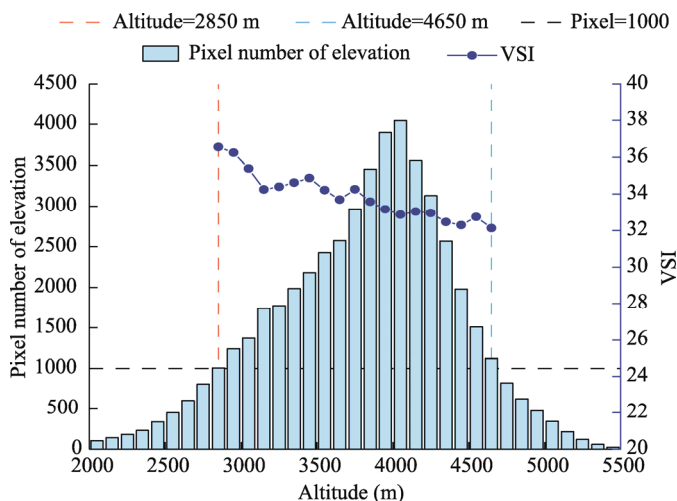


Fig. 6 VSI variation with altitude in the QMNP

3.2.3 Resistance of different types of ecosystems

The QMNP ecosystems are diverse and complex, and include forests, shrublands, grasslands, wetlands, and desert ecosystems. By overlapping the spatial distribution of VSI with the distribution of ecosystems, we can determine the resistance of different types of ecosystems. In general, different types of ecosystems in the QMNP have significantly different resistances against climate variability, which are manifested in the differences between areas of different ecosystem types, as well as the differences between different areas of the same type of ecosystem. Box plots were used to represent the value ranges and medians of VSI in different ecosystems (Fig. 7). This method excludes the effect of outliers and describes the discrete distribution of the data in a relatively stable manner.

Grasslands are a widely distributed ecosystem in the QMNP and cover an area of approximately $31,100\text{ km}^2$. Grassland ecosystem resistance was typically high. The average VSI for grasslands was 34.600, with temperate grasslands between 35.000 and 55.000, desert grasslands between 25.000 and 45.000, and alpine grasslands between 20.000 and 45.000. The proportion of grassland with VSI less than 20.000 was 3.69%; between 20.000 and 30.000 was 24.35%, between 30.000 and 40.000 was 45.64%, between 40.000 and 50.000 was 21.84%, and greater than 50.000 was 4.47%. From a spatial perspective, the overall grassland VSI of the

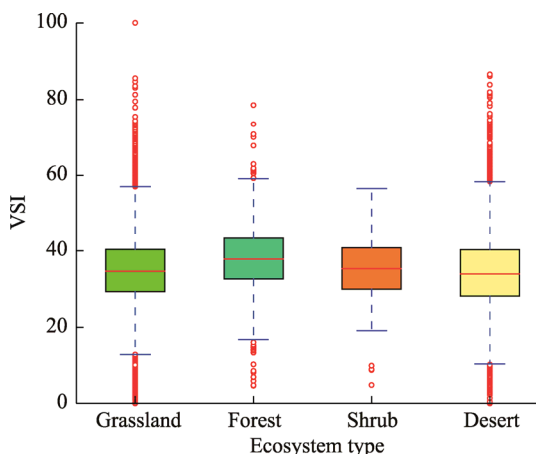


Fig. 7 Box-plot diagram of VSI in different ecosystems in the QMNP. The upper and lower limits of the box indicate the 75th and 25th percentile values, respectively; the horizontal line in each box represents the median of the distributions; and the upper and lower whiskers show the 95th and 5th percentile values, respectively; the red circles indicate outliers.

western section of the QMNP was generally less than 40.000, whereas the VSI value of the middle section was concentrated around 40.000–50.000. In general, the grassland VSI values of the western and middle sections were higher than those of the eastern section. Accordingly, the resistance of the grassland ecosystem in the middle and western sections was weaker than that in the eastern section.

The total area of forest ecosystems in the QMNP is approximately 2300 km² and is mainly distributed in the middle and eastern sections. The resistance of forest ecosystems was generally strong, with an average VSI value of 34.600. Areas with a VSI value less than 30.000 accounted for 14.91% of the total forest ecosystem, 30.000–40.000 accounted for 46.80%, 40.000–50.000 accounted for 31.06%, and greater than 50.000 accounted for 7.20%. Spatially, the resistance of forest ecosystems in the middle section was stronger than that in the eastern section, and the resistance of forest ecosystem at the edge of the QMNP was greater than that in the central area.

The QMNP also features four other types of ecosystem with smaller areas. First, the total area of shrub ecosystems in the QMNP is approximately 3000 km², mainly distributed in the eastern section. Areas with a VSI value less than 20.000 accounted for 2.16%, 20.000–30.000 accounted for 23.74%, 30.000–40.000 accounted for 44.24%, 40.000–50.000 accounted for 26.26%, and greater than 50.000 accounted for 3.60%. The VSI value of shrub ecosystems in the eastern section was lower than that in the middle section. Second, the total area of desert ecosystems with vegetation coverage greater than 5.00% was approximately 10,600 km². Areas with a VSI value less than 20.000 accounted for 5.44%, 20.000–30.000 accounted for 26.49%, 30.000–40.000 accounted for 42.33%, 40.000–50.000 accounted for 19.22%, and greater than 50.000 accounted for only 6.52%. The high and low-value areas were staggered, indicating that the resistance of desert ecosystems fluctuated greatly. Third, wetland ecosystems typically had VSI values between 30.000–50.000, with the corresponding area accounting for 65.72% of the total area, indicating strong resistance. Fourth, 76.56% of the ice and snow ecosystems had VSI values between 20.000–50.000, which also indicated strong resistance.

3.2.4 Resistance to different climate disturbances

To analyze ecosystem resistance to different climatic factors, we evaluated the relative contributions of temperature, precipitation, and solar radiation to the sensitivity of vegetation, and combined the three climatic factors with their separate VSI bands. Figure 8 showed the results obtained using the RGB (red, green, and blue) band synthesis method.

Figure 8 illustrated the complex and non-linear spatial patterns in the relative importance of the three climatic factors (temperature, precipitation, and solar radiation) to vegetation

sensitivity. The grasslands in the western section were mostly green, indicating that precipitation variability played a crucial role in the stability of grassland ecosystems in this area. However, the grasslands in the middle section were mostly yellow, indicating that they were affected by both precipitation and temperature variability. The grasslands in the eastern section were more purple, indicating that the temperature and solar radiation variability had an effect on the stability of grassland ecosystems in this area. Therefore, the overall grassland ecosystems were influenced by the combined effects of temperature, precipitation, and solar radiation.

The areas of forest ecosystems were mainly purple and blue, indicating the dual effects of temperature and solar radiation variability. The distribution of shrub ecosystems was mostly yellow and green, indicating that they were affected by both temperature and precipitation variability. The distribution of desert ecosystems in the western section was mostly green, indicating that precipitation variability was the main climatic factor, whereas the distribution areas in the middle and eastern sections were mostly purple, indicating that temperature and solar radiation variability influenced the stability of desert ecosystems in these regions.

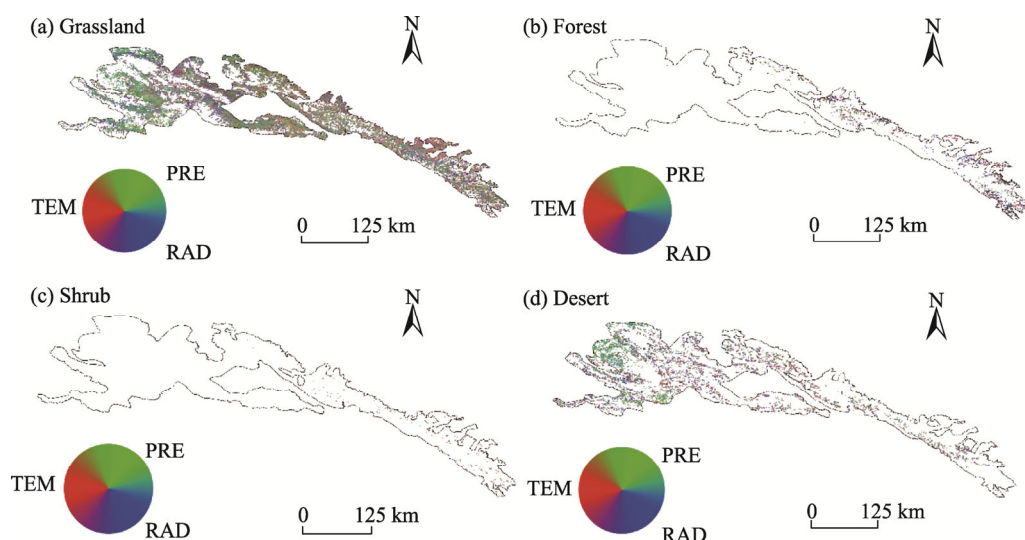


Fig. 8 RGB (red, green, and blue) composite of climate factors to ecosystem vegetation in the QMNP. Red, green, and blue represent temperature, precipitation, and solar radiation, respectively.

4 Discussion

The geographical heterogeneity of the QMNP is significant. In addition to the large undulations of the terrain, there is more precipitation and vegetation coverage in the eastern section than in the western section. Furthermore, there are significant latitude and altitudinal gradient changes in the ecosystems. The QMNP has various types of landforms, a large topographic drop, and differences in climate within different types of units. In addition, there are differences in the vertical band of spectrum of vegetation in the eastern, central, and western sections, and the vegetation distribution on the southern and northern slopes of the mountains is also difference, which leads to complex changes in climate and vegetation. The superposition of these differences provides each region with unique conditions. This complex and mosaic geospatial differentiation determines the spatial differentiation of ecosystem stability to a certain extent and the heterogeneity and non-linearity of ecosystem response to climate change.

Most ecosystems are widely distributed in the QMNP, but there are differences in the controlling climatic factors for the stability of similar ecosystems in different regions. This shows that there is a difference in the climate-ecosystem relationship at the regional and global levels. Moreover, owing to the interaction between different climatic factors, it is difficult for a single

climatic factor to exert a linear influence on ecosystem stability. Chaos theory holds that complex dynamic systems consist of intertwined links and, therefore, cannot be explained by a single relationship (Britannica, 2023). Fractals are chaotic on a spatial scale and can also reveal self-similarities in complex natural systems. The staggered and mosaic nature of the distribution of ecosystems in the QMNP produces irregular and non-linear patterns at the regional and global levels, and the impact of climate change on ecosystems is complex and non-linear.

The hysteresis effect of vegetation further increases the uncertainty of ecosystem responses to climate change to a certain extent. The hysteresis effect, also known as the vegetation memory effect, implies that as vegetation grows slowly, its response to climate change tends to be delayed (Harris et al., 2014). Therefore, vegetation growth depends not only on current disturbances but also on the residual effects of past climatic conditions. This memory effect should be considered when assessing vegetation responses to short-term climate variability (Seddon et al., 2016). Vegetation in arid areas usually has a strong ability to cope with the disturbance of climatic factors; therefore, the vegetation in these areas usually shows a strong memory effect (Han et al., 2021).

Although hysteresis of the response is common, there are often some differences at different scales. For example, most areas of vegetation in the low latitudes of the northern and southern hemispheres (30°S–30°N) have a lag time of over one month for temperature. The arid and semi-arid areas in the northern hemisphere have a lag time of approximately one month for precipitation. Vegetation in the high latitudes of the northern hemisphere has a lag time of approximately one month to solar radiation. A study of 32 major cities in China found that the memory effect was the longest and strongest for humidity, whereas evaporation was the shortest and weakest. Furthermore, the memory effect of precipitation and solar radiation on vegetation is stronger in southern China than in northern China (Tang et al., 2021).

The changes in gross primary productivity (GPP) in the central Qilian Mountains region are mainly caused by temperature, while in the west and east, they are mainly caused by drought. Furthermore, the response of GPP to temperature, precipitation, and solar radiation varies with season and biome (Xu, 2019). Differences in timescales affect the correlation between vegetation and climate. In addition to being used to determine lag time, different timescales are commonly used to determine the dominant timescale of drought response. The timescale with the highest correlation is an effective indicator of drought resistance (Xu, 2018). This study found that vegetation in the growing season has different requirements for temperature and precipitation in different months; therefore, the sensitivity to temperature and precipitation is also different. Studies on the relationship between vegetation cover and climate change in China over the past 20 years have also reached a similar conclusion; that is, the maximum correlation coefficient between vegetation cover and climate factors of different land types is delayed by one month (Sun et al., 2020).

The climate of the QMNP belongs to the continental alpine and semi-humid mountain climate, the vegetation grows slowly, and the response time of vegetation to climate variation will be longer. Therefore, this study appropriately examined vegetation resistance to the three climate variables using the one-month lag EVI. However, the monthly temperature and precipitation data used in this study were obtained from the National Science and Technology Infrastructure Platform-National Earth System Science Data Center. Owing the limited distribution of meteorological stations in the QMNP, the data of the center have not been revised, and it needs to be improved in the future. The memory effects of different types of ecosystems and vegetation in different spaces of the same type of ecosystem on the climate are different, and homogenization will lead to a certain degree of distortion. Future research is needed to clarify the differences in the lag of different ecosystem responses to climate change.

5 Conclusions

Climate change has been identified as the most extensive and persistent disturbance of ecosystems in arid areas, driving changes in the NDVI and the overall stability of vegetation.

Ecosystem responses to climate change are complex phenomena that are affected by multiple biological and abiotic factors. This study examined ecosystem responses to short-term climate variability in the QMNP, focusing on the heterogeneity and non-linearity of ecosystem stability. The findings show that while the ecosystems of the QMNP have a high level of resistance to climate variability over the past 20 years, there is significant heterogeneity and non-linearity in the degree of resistance of different ecosystems, driven by both the spatial distribution of ecosystems and the influence of different climatic factors on different ecosystems.

Examining the heterogeneity of ecosystem resistance has deepened our understanding of the non-linear relationship between ecosystems and climate change. The climate and ecosystems are complex systems. As such, the relationship between ecosystems and climate change is inherently non-linear and uncertain, making it difficult to predict future states. The characteristics of non-linear ecosystem responses to climate change include: (1) the controlling climatic factors of the same ecosystems vary in different geographical locations; (2) the interaction between different climatic factors lead to variations in the weights that affect ecosystem stability vary and are difficult to determine; and (3) the hysteresis effect of vegetation, which adds to the uncertainty of ecosystem responses to climate change.

Acknowledgements

This research was supported by the National Key Research and Development Program of China (2019YFC0507402).

References

Bader M Y, van Geloof I, Rietkerk M. 2007. High solar radiation hinders tree regeneration above the alpine treeline in northern Ecuador. *Plant Ecology*, 191(1): 33–45.

Bai Y F, Han X G, Wu J G, et al. 2004. Ecosystem stability and compensatory effects in the Inner Mongolia grassland. *Nature*, 431(7005): 181–184.

Britannica. 2023. Encyclopedia Britannica. [2023-01-02]. <https://www.britannica.com>.

Cai W H, Yang Y Z, Yang J, et al. 2018. Topographic variation in the climatic change response of a larch forest in Northeastern China. *Landscape Ecology*, 33(11): 2013–2029.

Chen C, He B, Yuan W P, et al. 2019. Increasing interannual variability of global vegetation greenness. *Environmental Research Letters*, 14(12): 124005, doi: 10.1088/1748-9326/ab4ffc.

Chen F H, Chen J, Huang W. 2021. Weakened East Asian summer monsoon triggers increased precipitation in Northwest China. *Science China Earth Sciences*, 64: 835–837.

Chen S Y, Zhang Y L, Wu Q L, et al. 2021. Vegetation structural change and CO₂ fertilization more than offset gross primary production decline caused by reduced solar radiation in China. *Agricultural and Forest Meteorology*, 296: 108207, doi: 10.1016/j.agrformet.2020.108207.

Chen Y N, Chen Y P, Zhu C G, et al. 2019. The concept and mode of ecosystem sustainable management in arid desert areas in northwest China. *Acta Ecologica Sinica*, 39(20): 7410–7417. (in Chinese)

De Keersmaecker W, Lhermitte S, Tits L, et al. 2015. A model quantifying global vegetation resistance and resilience to short - term climate anomalies and their relationship with vegetation cover. *Global Ecology and Biogeography*, 24(5): 539–548.

Du J, He Z B, Chen L F, et al. 2021. Impact of climate change on alpine plant community in Qilian Mountains of China. *International Journal of Biometeorology*, 65(11): 1849–1858.

Du Q Q, Sun Y F, Guan Q Y, et al. 2022. Vulnerability of grassland ecosystems to climate change in the Qilian Mountains, northwest China. *Journal of Hydrology*, 612: 128305, doi: 10.1016/j.jhydrol.2022.128305.

Gao X, Huang X X, Lo K W, et al. 2021. Vegetation responses to climate change in the Qilian Mountain Nature Reserve, Northwest China. *Global Ecology and Conservation*, 28: e01698, doi: 10.1016/j.gecco.2021.e01698.

Garcia-Palacios P, Gross N, Gaitán J, et al. 2018. Climate mediates the biodiversity–ecosystem stability relationship globally. *Proceedings of the National Academy of Sciences*, 115(33): 8400–8405.

Gou X, Hou F, Li Y, et al. 2022. Report on the Scientific Study of Ecosystem Change in Qilian Mountains. Beijing: Science Press.

Gu J F, Zhou Z X, Li Z K, et al. 2017. Photosynthetic properties and potentials for improvement of photosynthesis in pale green leaf rice under high light conditions. *Frontiers in Plant Science*, 8: 1082, doi: 10.3389/fpls.2017.01082.

Han F F, Yan J J, Ling H B. 2021. Variance of vegetation coverage and its sensitivity to climatic factors in the Irtysh River basin. *PeerJ*, 9: e11334, doi: 10.7717/peerj.11334.

Harris A, Carr A S, Dash J. 2014. Remote sensing of vegetation cover dynamics and resilience across southern Africa. *International Journal of Applied Earth Observation and Geoinformation*, 28: 131–139.

He Y, Yan H W, Ma L, et al. 2020. Spatiotemporal dynamics of the vegetation in Ningxia, China using MODIS imagery. *Frontiers of Earth Science*, 14(1): 221–235.

Hillebrand H, Donohue I, Harpole W S, et al. 2020. Thresholds for ecological responses to global change do not emerge from empirical data. *Nature Ecology & Evolution*, 4(11): 1502–1509.

Hisano M, Searle E B, Chen H Y. 2018. Biodiversity as a solution to mitigate climate change impacts on the functioning of forest ecosystems. *Biological Reviews*, 93(1): 439–456.

Huang K, Xia J Y. 2019. High ecosystem stability of evergreen broadleaf forests under severe droughts. *Global Change Biology*, 25(10): 3494–3503.

Jiang C, Zhang H Y, Tang Z P, et al. 2017. Evaluating the coupling effects of climate variability and vegetation restoration on ecosystems of the Loess Plateau, China. *Land Use Policy*, 69: 134–148.

Jiang P, Ding W G, Yuan Y, et al. 2022. Interannual variability of vegetation sensitivity to climate in China. *Journal of Environmental Management*, 301: 113768, doi: 10.1016/j.jenvman.2021.113768.

Joly F, Sabatier R, Tatin L, et al. 2022. Adaptive decision-making on stocking rates improves the resilience of a livestock system exposed to climate shocks. *Ecological Modelling*, 464: 109799, doi: 10.1016/j.ecolmodel.2021.109799.

Kang W P, Liu S L, Chen X, et al. 2022. Evaluation of ecosystem stability against climate changes via satellite data in the eastern sandy area of northern China. *Journal of Environmental Management*, 308: 114596, doi: 10.1016/j.jenvman.2022.114596.

Kerr L, Cadin S, Secor D. 2010. The role of spatial dynamics in the stability, resilience, and productivity of an estuarine fish population. *Ecological Applications*, 20(2): 497–507.

Li J, Yu S Y, Liu L. 2020. Determining the dominant factors determining the variability of terrestrial ecosystem productivity in China during the last two decades. *Land Degradation & Development*, 31(15): 2131–2145.

Li S C, Su S, Liu Y X, et al. 2022. Effectiveness of the Qilian Mountain Nature Reserve of China in reducing human impacts. *Land*, 11(7): 1071, doi: 10.3390/land11071071.

Liu H Y, Mi Z R, Lin L, et al. 2018. Shifting plant species composition in response to climate change stabilizes grassland primary production. *Proceedings of the National Academy of Sciences*, 115(16): 4051–4056.

Liu J R, Zhao J, Wang J B. 2021a. Response of vegetation cover to drought in the Qilian Mountains Region from 2001 to 2016. *Pratacultural Science*, 38: 419–431. (in Chinese)

Liu L Y, Gou X H, Zhang F, et al. 2021b. Effects of warming on radial growth of *Picea crassifolia* in the eastern Qilian Mountains, China. *The Journal of Applied Ecology*, 30: 3576–3584.

Liu Y Y, Wang Q, Zhang Z Y, et al. 2019. Grassland dynamics in responses to climate variation and human activities in China from 2000 to 2013. *Science of the Total Environment*, 690: 27–39.

Ma Y R, Guan Q Y, Sun Y F, et al. 2022. Three-dimensional dynamic characteristics of vegetation and its response to climatic factors in the Qilian Mountains. *CATENA*, 208: 105694, doi: 10.1016/j.catena.2021.105694.

Malfasi F, Cannone N. 2020. Climate warming persistence triggered tree ingression after shrub encroachment in a high alpine tundra. *Ecosystems*, 23(8): 1657–1675.

Malhi Y, Franklin J, Seddon N, et al. 2020. Climate change and ecosystems: Threats, opportunities and solutions. *Philosophical Transactions of the Royal Society B*, 375: 20190104, doi: 10.1098/rstb.2019.0104.

Marchal J, Cumming S G, McIntire E J. 2020. Turning down the heat: Vegetation feedbacks limit fire regime responses to global warming. *Ecosystems*, 23(1): 204–216.

Miao L J, Sun Z L, Ren Y J, et al. 2021. Grassland greening on the Mongolian Plateau despite higher grazing intensity. *Land Degradation & Development*, 32(2): 792–802.

Ministry of Ecology and Environment of the People's Republic of China. 2021. Technical specification for investigation and assessment of national ecological status—Ecosystem quality assessment (HJ 1172—2021). [2022-06-10]. <https://www.mee.gov.cn/ywqz/fgbz/bz/bzwb/stzl/202106/W020210910456717871866.pdf>.

Morin X, Fahse L, Jactel H, et al. 2018. Long-term response of forest productivity to climate change is mostly driven by change in tree species composition. *Scientific Reports*, 8(1): 5627, doi: 10.1038/s41598-018-23763-y.

Nolan C, Overpeck J T, Allen J R, et al. 2018. Past and future global transformation of terrestrial ecosystems under climate change. *Science*, 361(6405): 920–923.

Pennekamp F, Pontarp M, Tabi A, et al. 2018. Biodiversity increases and decreases ecosystem stability. *Nature*, 563(7729): 109–112.

Piao S L, Liu Q, Chen A P, et al. 2019. Plant phenology and global climate change: Current progresses and challenges. *Global*

Change Biology, 25(6): 1922–1940.

Qian D W, Cao G G, Du Y G, et al. 2019. Impacts of climate change and human factors on land cover change in inland mountain protected areas: A case study of the Qilian Mountain National Nature Reserve in China. *Environmental Monitoring and Assessment*, 191: 486, doi: 10.1007/s10661-019-7619-5.

Qu S, Wang L C, Lin A, et al. 2020. Distinguishing the impacts of climate change and anthropogenic factors on vegetation dynamics in the Yangtze River Basin, China. *Ecological Indicators*, 108: 105724, doi: 10.1016/j.ecolind.2019.105724.

Rogora M, Frate L, Carranza M, et al. 2018. Assessment of climate change effects on mountain ecosystems through a cross-site analysis in the Alps and Apennines. *Science of the Total Environment*, 624: 1429–1442.

Sánchez-Pinillos M, Leduc A, Ameztegui A, et al. 2019. Resistance, resilience or change: post-disturbance dynamics of boreal forests after insect outbreaks. *Ecosystems*, 22(8): 1886–1901.

Seddon A W, Macias-Fauria M, Long P R, et al. 2016. Sensitivity of global terrestrial ecosystems to climate variability. *Nature*, 531(7593): 229–232.

Seixas H T, Brunsell N A, Moraes E C, et al. 2022. Exploring the ecosystem resilience concept with land surface model scenarios. *Ecological Modelling*, 464: 109817, doi: 10.1016/j.ecolmodel.2021.109817.

Shang J X, Zhang Y, Peng Y, et al. 2022. Climate change drives NDVI variations at multiple spatiotemporal levels rather than human disturbance in Northwest China. *Environmental Science and Pollution Research*, 29(10): 13782–13796.

Sloat L L, Gerber J S, Samberg L H, et al. 2018. Increasing importance of precipitation variability on global livestock grazing lands. *Nature Climate Change*, 8(3): 214–218.

Stanimirova R, Arévalo P, Kaufmann R K, et al. 2019. Sensitivity of global pasturelands to climate variation. *Earth's Future*, 7(12): 1353–1366.

Sun G Q, Guo B, Zang W Q, et al. 2020. Spatial–temporal change patterns of vegetation coverage in China and its driving mechanisms over the past 20 years based on the concept of geographic division. *Geomatics, Natural Hazards and Risk*, 11(1): 2263–2281.

Tang W X, Liu S G, Kang P, et al. 2021. Quantifying the lagged effects of climate factors on vegetation growth in 32 major cities of China. *Ecological Indicators*, 132: 108290, doi: 10.1016/j.ecolind.2021.108290.

van Rooijen N M, De Keersmaecker W, Ozinga W A, et al. 2015. Plant species diversity mediates ecosystem stability of natural dune grasslands in response to drought. *Ecosystems*, 18(8): 1383–1394.

Wang Y H, Li D H, Lu G Y, et al. 2022. Characteristics of climate change in Qilian Mountains and its impact on water resources. *Journal of Applied Ecology*, 33: 2805–2812.

Weiskopf S R, Rubenstein M A, Crozier L G, et al. 2020. Climate change effects on biodiversity, ecosystems, ecosystem services, and natural resource management in the United States. *Science of the Total Environment*, 733: 137782, doi: 10.1016/j.scitotenv.2020.137782.

Woolway R I, Kraemer B M, Linters J D, et al. 2020. Global lake responses to climate change. *Nature Reviews Earth & Environment*, 1(8): 388–403.

Xu Y F, Yang J, Chen Y N. 2016. NDVI-based vegetation responses to climate change in an arid area of China. *Theoretical and Applied Climatology*, 126(1): 213–222.

Yuan Y, Bao A M, Liu T, et al. 2021. Assessing vegetation stability to climate variability in Central Asia. *Journal of Environmental Management*, 298: 113330, doi: 10.1016/j.jenvman.2021.113330.

Zhang L F, Qiao N, Huang C P, et al. 2019. Monitoring drought effects on vegetation productivity using satellite solar-induced chlorophyll fluorescence. *Remote Sensing*, 11(4): 378, doi: 10.3390/rs11040378.

Zhang S R, Bai X Y, Zhao C W, et al. 2022. Limitations of soil moisture and formation rate on vegetation growth in karst areas. *Science of the Total Environment*, 810: 151209, doi: 10.1016/j.jenvman.2021.113330.

Zhang T, Zhang Y J, Xu M J, et al. 2016. Ecosystem response more than climate variability drives the inter-annual variability of carbon fluxes in three Chinese grasslands. *Agricultural and Forest Meteorology*, 225: 48–56.

Zhao Y C, Wang X Y, Novillo C J, et al. 2019. Remotely sensed albedo allows the identification of two ecosystem states along aridity gradients in Africa. *Land Degradation & Development*, 30(12): 1502–1515.

Zhou Y K, Fan J F, Wang X Y. 2020. Assessment of varying changes of vegetation and the response to climatic factors using GIMMS NDVI3g on the Tibetan Plateau. *PLoS One*, 15(6): e0234848, doi: 10.1371/journal.pone.0234848.

Zhu Y K, Zhang J T, Zhang Y Q, et al. 2019. Responses of vegetation to climatic variations in the desert region of northern China. *CATENA*, 175: 27–36.